

Causes of PCV pressure increase at Unit-3 from March 11th to 12th, 2011

This document was prepared based on the proposal and evaluation by TEPCO Systems Corporation concerning the PCV pressure behavior of Unit-3 from March 11th to 12th in connection with the thermal stratification in the Unit-3 suppression chamber pool, which is listed as “Unit-3/Issue-3” in Attachment 2.

1. Background

At Unit-3, the steam generated by the decay heat in the reactor was transferred to the suppression chamber (S/C) pool via safety-relief valves (SRVs) and in parallel the reactor core isolation cooling system (RCIC) was discharging the steam it had bled to the S/C. Certainly this contributed to the PCV pressure increase, but the PCV pressure increase rate was higher than the rate anticipated when the steam generated by the decay heat in the reactor vessel was transferred to the S/C and the S/C pool water temperature was homogeneously increased.

This incident could be explained by the scenario with the possibility that the S/C pool water temperature near the outlet of the RCIC turbine exhaust steam discharge line increases; the high temperature water spreads circumferentially in the S/C pool water surface area forming thermal stratification; and consequently, higher temperature of the water surface caused a higher pressure increase in the PCV than the case of the uniform temperature increase in the S/C[1]. Another possible scenario could be obtained from the relationship between the measured pressures of the PCV drywell (D/W) and S/C: steam leaks from the reactor pressure vessel (RPV) to the D/W caused the D/W pressure increase, since the D/W pressure was higher than the S/C pressure.

This document reports on the causes of PCV pressure increase estimated by trend analysis of measured values, reproducibility of measured values by the analysis and a literature survey.

2. Estimation of the causes of PCV pressure increase based on the measured data from March 11th to 12th

Four sets of data measured during the accident are available for Unit-3. Figure 2-1 shows all these data. They are: (i) the data made publically available on November 30th, 2012 (①)[2]; (ii) Unit-3 plant data readings (②)[3]; (iii) chart data (③)[4]; and (iv) the data on the transient recorder (④). The RPV pressures and SRV preset pressures correspond to the

right Y-axis, and other data correspond to the left Y-axis. In the following sections, the causes of PCV pressure increase were estimated by the trend analysis of these data.

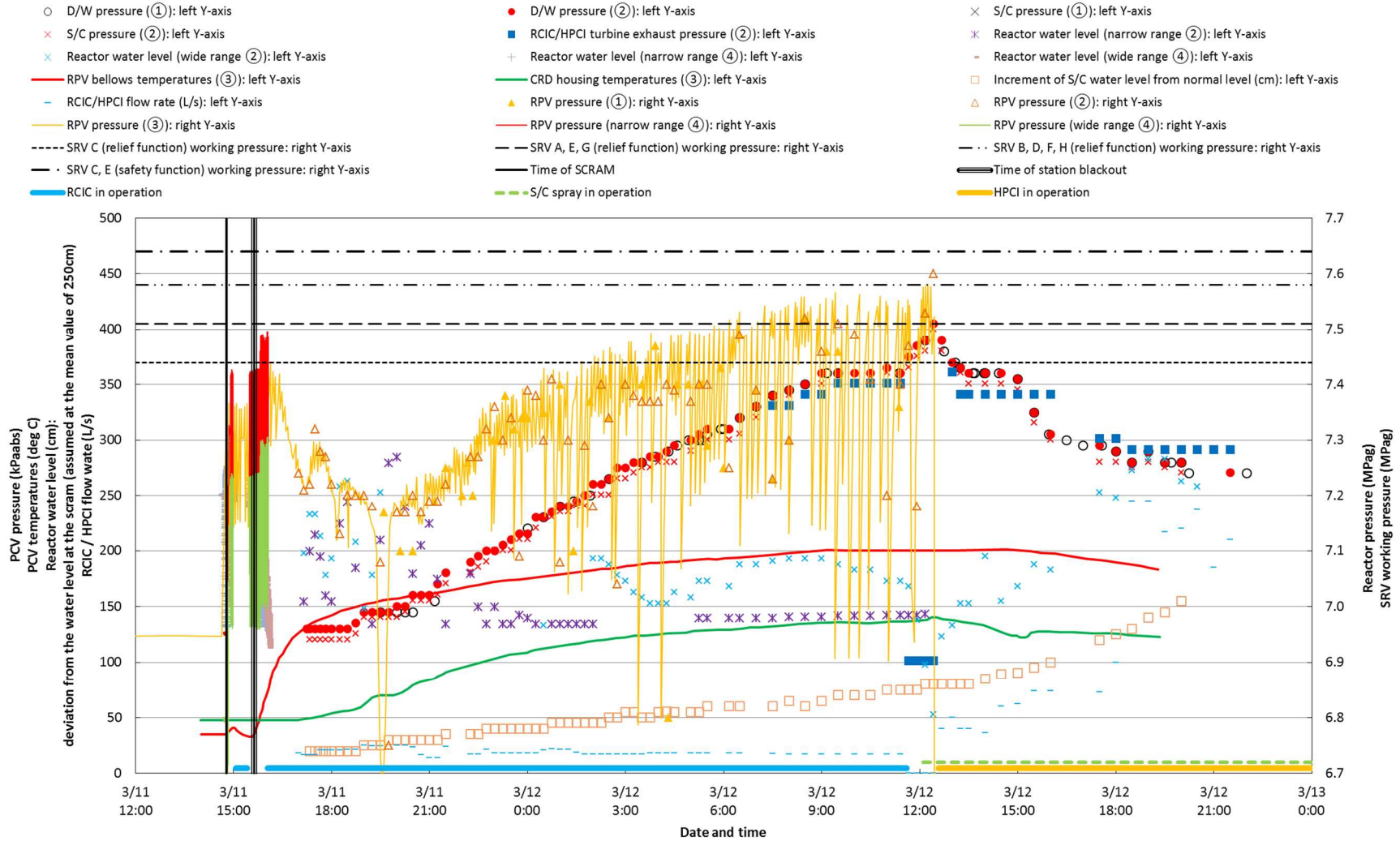


Figure 2-1 Data measured on March 11th and 12th

(HPCI, high pressure coolant injection system; CRD, control rod drive; all other acronyms are as explained in the text)

2.1. Estimation based on the RPV pressures and water levels

As seen in Figure 2-1, while the PCV pressure was increasing, the RPV pressure increased gradually in ups and downs hinting at SRV operations. Further the RPV pressures exceeded the SRV working pressures, while increasing. Therefore, the SRVs are considered to have worked. Consequently, steam having the energy corresponding to the decay heat is considered to have been flowing into the S/C, being integrated with the energy from the extracted steam for the RCIC operation.

The reactor water level changed in the range of about -1.2 to +0.3m relative to the water level at the reactor scram. It can be considered that the water level did not reach the main steam line piping elevation. This comes from the fact that the RCIC was being operated to maintain the reactor water level as constantly as possible by adjusting the amount of water to be injected. Therefore, the energy transfer to the S/C via unforeseen paths is hard to conceive, such as direct flows of reactor water to the S/C via the SRVs or RCIC turbine.

To sum up, these data are not useful to explain the causes of the PCV pressure increase at a higher rate than anticipated from the decay heat.

2.2. Estimation based on the D/W temperatures

As seen in Figure 2-1, the in-PCV air temperatures were recorded on the chart at two locations: at the RPV bellows position (below the bulk head plate) and at the CRD housing. Temperatures increased almost monotonically after all the AC power sources had been lost (SBO) until the RPV depressurization, to about 200 deg C at the bellows position and about 140 deg C at the CRD housing position. For each location, the data were collected at two circumferential points, but the difference between these two points was small (Figure 2-1 shows only one of them for simplicity). This means, the situation was such that no big temperature distribution could be generated circumferentially.

Such D/W temperature increases can be considered to have been caused by: the heat transfer from the RPV; the steam inflow from the exhaust via the S/C; and the leaks in gaseous or liquid phases from the RPV to the D/W. Concerning the leaks from the RPV to the D/W, circumferential temperature distributions may be formed subject to the leak position, but no such indication is recognized. It is too early to conclude that no leaks occurred from the RPV to the D/W, but it is at least probable that no leaks occurred around the subject points of the measurement which may cause circumferential temperature distributions.

2.3. Estimation based on the D/W pressures and S/C pressures

The PCV pressure in Figure 2-1 increased faster than anticipated from the decay heat. Thermal stratification in the S/C pool water might be the reason [1]. Meanwhile, the D/W

pressure was higher than the S/C pressure, hinting at a possibility of steam leaks from the RPV to the D/W.

Figure 2-2 shows the difference between the measured D/W and S/C pressures. It also shows the pressure difference anticipated when either the D/W or the S/C pressure changes for some reason (increase or decrease), assuming integrity (no gaps) of the vent tube that connects the D/W and S/C: (i) If the D/W pressure increases for some reason (e.g., leaks from the RPV) the water in the vent tube is pressed downward to the bottom end, its inner side (D/W side) and outer side (S/C side) form a level difference and the D/W pressure becomes higher than the S/C pressure by the amount of this water head. Since the S/C water level is increasing, the pressure difference is anticipated to increase gradually; (ii) on the contrary, if the S/C pressure increases for some reason, the pressure difference between the D/W and S/C is anticipated to change between about -3 to 0kPa on the graph by the vacuum breaker function until the S/C spray starts. Once the S/C spray starts, the S/C pressure decreases, the D/W pressure becomes comparatively higher, the water level in the vent tube is lowered and eventually the similar pressure difference is expected to be achieved as in the case when the initial pressure increase starts in the D/W.

However, the measured pressure difference agrees with neither of the pressure differences anticipated, that is, when the D/W pressure or the S/C pressure increases for some reason. Therefore, the measured pressure difference does not tell which of the two, the D/W or the S/C, was the cause of pressure changes.

Errors in the measured values could be a cause of discrepancy between the measured pressure difference and the anticipated value. Both the D/W and S/C pressure indicators are the diaphragm type (with a disc-shaped pressure sensor bending at right angles), and the object to be measured (the reference material for the pressure measurement) is nitrogen gas for the D/W pressure indicator and water for the S/C pressure indicator. At the time of the accident (till March 23rd, 2011), the D/W and S/C pressure indicator readings were checked on the accident management panel. Figure 2-3 illustrates respective system diagrams.

It has been known that these pressure indicators are susceptible to environmental temperatures, radiation, humidity, etc. causing errors. When the indicators are powered by batteries, insufficient battery power can also cause errors. Furthermore, the S/C pressure indicator may underestimate the actual pressure, if the water level in the pipe upstream from the indicator is decreased due to effects of the accident; under normal conditions it is supposed to be kept constant at that of the condensing water chamber. In reality, it is difficult to determine the extent of the errors that the pressure indicators had at the time of the accident.

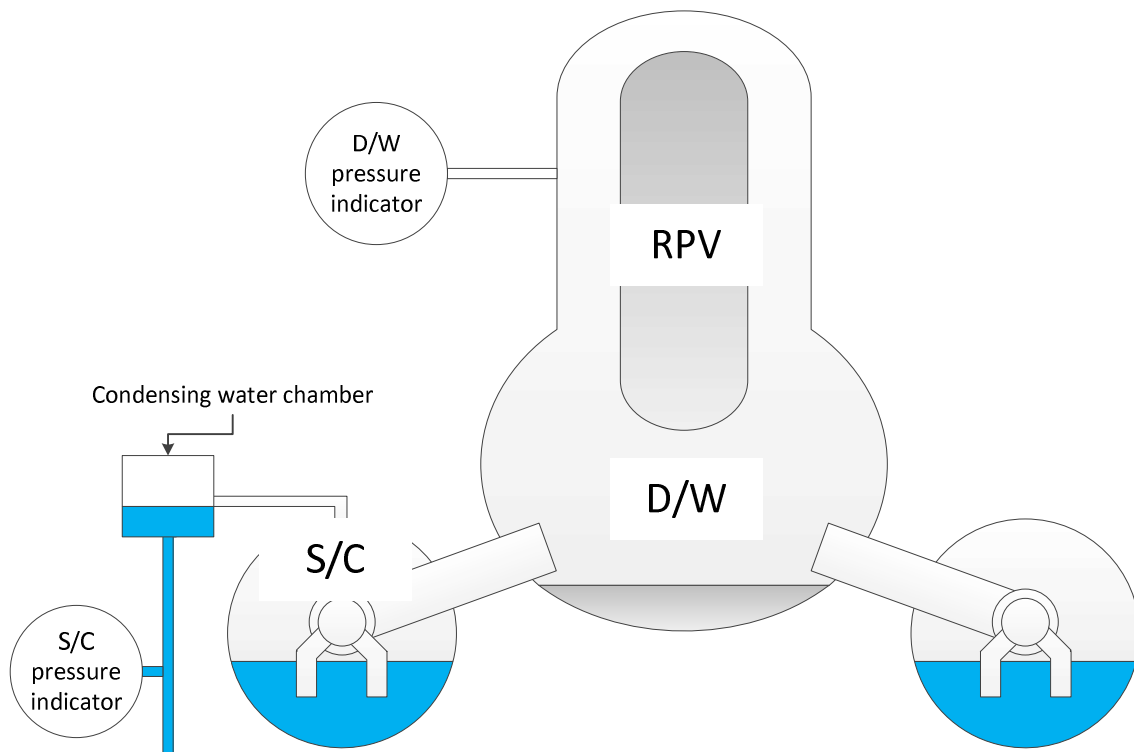


Figure 2-3 System diagram (outline) of PCV pressure indicators

3. PCV pressure behavior evaluation by analysis

The previous section rationalized that the measured data could not be used to determine which of the two, the D/W or S/C, caused the PCV pressure increase. This section attempted to reproduce the PCV pressure increase from March 11th to 12th, 2011, by the analysis. In the analysis, the general thermal-hydraulic analysis code GOTHIC Version 8.1(QA) was used.

The thermal stratification in the S/C pool is a very complicated phenomenon to model, and it is still too early to evaluate in detail the temperature distributions in the S/C. Further efforts are needed to this end, including improvement of the modeling method. In the current evaluation, therefore, the reproducibility of measured data by analysis was checked in the case of leaks from the RPV to the D/W.

3.1. Geometry for analysis

Figure 3-1 gives the geometry for the GOTHIC analysis. In the geometry both the D/W and S/C were modeled in order to check the reproducibility of D/W and S/C pressure behaviors. The D/W in particular was divided into six regions to take into account the temperature distributions inside it. They were the D/W lower region (up to the bottom end of the cylindrical portion), pedestal region, D/W middle region (from the bottom end of the cylindrical portion

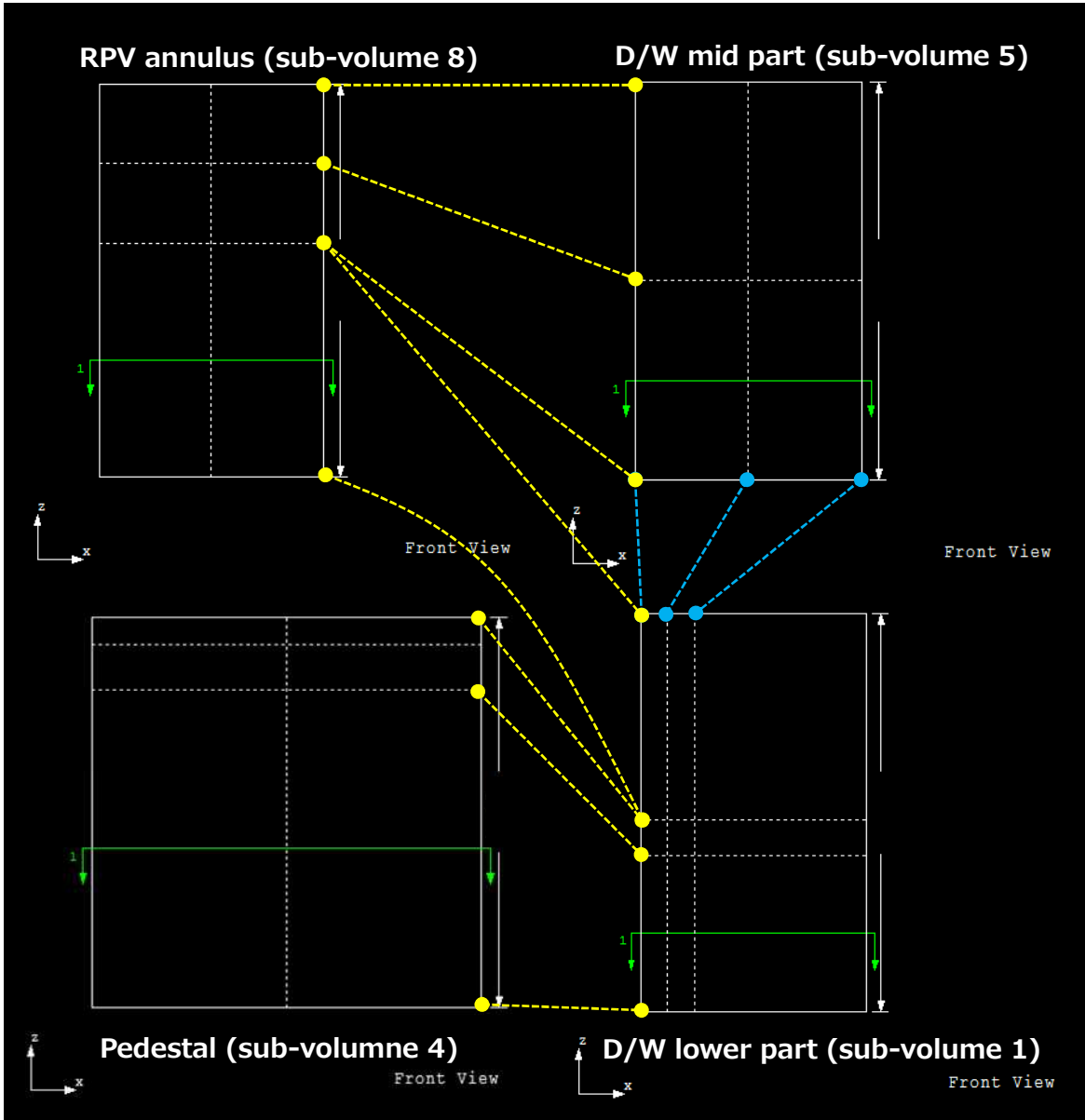
to the top end of the shield wall), D/W upper region (from the top end of the shield wall to the bulk head plate), D/W top head region, and RPV annulus region.

The D/W lower region, pedestal region, D/W middle region, and RPV annulus region were further divided into sub-regions (sub-volumes), as seen in Figure 3-2, in order to simulate counter-currents in the vertical direction in the region. In the circumferential direction no division was made, based on the judgement that it was unnecessary, because the measured D/W air temperatures had no big discrepancy in the circumferential direction.

The S/C was modeled in a single region. The relationship between the S/C water level and volumetric fraction was provided so that the water level and water volume in the torus configuration could be considered in the analysis.

The vent tube was modeled in order to check the water level behavior in it. The reactor well and reactor building were modeled to evaluate their influence on the D/W air temperature distributions due to heat loss of the D/W by being cooled through the PCV shell or concrete structures.

The RPV wall was given as the temperature boundary condition to consider its effect, while the steam inflow to the S/C from the SRVs or RCIC exhaust, and the leaks to the D/W were given as flow rate boundary conditions. The S/C spray flow rate and droplet diameters were set as adjustable parameters in the model.



※ The white broken lines are the division lines of sub-volumes, the yellow broken lines show the sub-volumes at the same elevation (they differ in the radial direction positions because of structures in between), and blue broken lines show the sub-volumes at the same elevation as well as at the same radial position. The green lines are cross-sectional lines in a top view and have no meaning for the present modeling.

Figure 3-2 Geometry for GOTHIC analysis (Setting of sub-volumes)

3.2. Conditions in the analysis

Reproducibility of the measured PCV pressure behavior was checked by analysis for cases of leaks from the RPV to the D/W. In order to confirm the effects of leak flow rates, different

leak flow rates from the RPV to D/W were analyzed. Table 3-1 presents the conditions for analysis.

Table 3-1 Key conditions for analysis (all cases)

Item		Set values	Notes
Time span of analysis	from	2011/3/11 15:40	At the time of SBO
	to	2011/3/12 20:00	
Initial temperatures	D/W	50 deg C	From chart data [4]
	S/C	30 deg C	From chart data [4]
	R/B	25 deg C	Assumed to be room temperature
Initial pressures	D/W, S/C	106kPa	Design value was used, as the chart data resolution was poor
	R/B	101kPa	Atmospheric pressure
Temperature boundary	RPV inner wall temperature	Saturation temperature at RPV pressure measured	-
Flow rate boundary	Steam inflow to S/C	Flow rate: steam generated by decay heat Temperature: Saturation temperature at S/C pressure measured	Steam generated by decay heat in the reactor was assumed to be flowing into the S/C. Decay heat was determined from the open source [2]
	S/C spray	Flow rate: 50m ³ /h Temperature: 20 deg C Droplet diameter: 2mm	Flow rate was set as reproducing S/C level measured, temperature was assumed as 20 deg C and droplet diameter as 2mm
	Multiplier to the flow rate RPV⇒D/W(*)	Case 1: 0 Case 2: 1 Case 3: 12	PCV pressure reproducibility to be checked under the following conditions Case 1: No leaks from RPV Case 2: Leaks conceivable from design were assumed Case 3: Big leaks beyond design were assumed

(*) A multiplier to be applied for the control bleedoff flow rate (3L/min/pump). In Case 3, it was adjusted so that the analysis results were in good agreement with the measured values.

3.3. Results of analysis

The analysis results of the Cases in Table 3-1 and the deliberations on the results are given below from 3.3.1 to 3.3.3. For Unit-2, which is the same reactor type as Unit-3, the PCV pressure showed an increase predictable from the decay heat over the time period of interest. For comparative assessment, the Unit-2 PCV pressure was also compared with the analysis results in the following sections.

3.3.1. Case 1

Case 1 did not assume leaks from the RPV to the D/W nor did it assume the pressure increase due to thermal stratification in the S/C. The results are shown in Figures 3-3 and 3-4. The analysis PCV pressures were far below the measured values. The analysis PCV pressures before the S/C spray showed a similar tendency with the measured values of Unit-2. Once the S/C spray started, the S/C pressure decreased temporarily by being cooled, and the D/W pressure decreased accordingly. Thereafter, the S/C pressure tended to increase again because of steam (energy) inflow from the RPV overwhelming the cooling effect by the S/C spray.

When the S/C spray started, the vent tube water level decreased temporarily. This is because the S/C temperatures decreased by the spray, the S/C pressure dropped below that of the D/W and the relatively high D/W pressure pushed down the vent tube water level. The S/C pressure increased thereafter and the vent tube water became level with the S/C water pool.

From the above, it was seen that the analysis PCV pressures were far below the measured values if no considerations were made to leaks from the RPV to the D/W or to the pressure increasing effect by the S/C pool water thermal stratification. It is necessary, therefore, to find some pressure increasing factors in order to reproduce analytically the PCV pressure increase at Unit-3.

3.3.2. Case 2

Case 2 assumed leaks in the liquid phase from the RPV to the D/W in the approximate amount of normal control bleedoff flow. The results are shown in Figures 3-5 and 3-6. As in Case 1, the analysis PCV pressures were far below the measured values. This is consistent with the previous study [4]. Upon occurrence of leaks in the liquid phase to the D/W, the liquid was changed to steam by flashing and the D/W pressure increased, but this increase was overwhelmed by the increase due to the S/C temperature increases. The S/C pressure started to increase earlier than the D/W pressure, as in Case 1. It should be noted that the

PCV pressure before the S/C spray was slightly closer to the measurements for Unit-2, when compared with the results of Case 1.

The S/C water level also showed a similar tendency with that of Case 1. The vent tube water level decreased due to the D/W pressure increase at the beginning, but it showed similar behavior later, as in Case 1, when the S/C pressures increased.

It could be concluded from the above that leaks in the liquid phase from the RPV to the D/W in the approximate amount of normal control bleedoff flow were not sufficient as a single factor to reproduce the measured PCV pressure increases of Unit-3.

3.3.3. Case 3

The results of Case 3 are shown in Figures 3-7 and 3-8. If large-sized leaks were assumed far exceeding the normal control bleedoff flow from the RPV to the D/W, it was possible to reproduce the PCV pressure increasing trend by the leaks only. However, the decreases of S/C pressures and D/W pressures after the S/C spray were too limited to reproduce the measured values. The calculated PCV pressures are considered to be more subject to decrease by the S/C spray than in the actual situation of the accident ^a, and it is still not possible to reproduce the measured values.

After the S/C spray, the D/W pressures decreased gradually to the level of S/C pressures. This is because the steam generation was reduced in the D/W caused by the reduced leak rate from the RPV to D/W due to the RPV depressurization, and because the D/W temperatures were lowered (lowered saturation pressures of steam) by the reduced heat transfer to the D/W due to the lowered saturation temperatures in the RPV. As a result, the D/W pressures became level with the S/C pressures.

^a In the current analysis, the droplets in the S/C spray were assumed to be 2mm in diameter. This 2mm is close to the diameter anticipated in the S/C spray at rated flow rate. The S/C spray flow rate in the accident was less than the rated value and therefore less in force. The droplet diameters would become bigger. When compared for one spray flow rate, spray with larger diameter droplets can cool less than the spray with smaller diameter droplets, because the total surface area of the larger diameter droplets is less than that of smaller diameter droplets. Since the current analysis assumed the ideal spray conditions, not considering the effect of enlarged diameter droplets, the PCV pressures are considered to be more subject to decrease by the S/C spray than in the actual situation of the accident.

The S/C water level changed at a slightly higher level than in Case 1. This is because the D/W pressures increased and pushed out the water in the vent tube to the S/C.

From the above it has been shown that large leaks from the RPV to the D/W as a single cause could explain the PCV pressure increasing behavior up until the time of the S/C spray, but they could not explain the PCV pressure decreasing behavior after the S/C spray.

In the analyses, it has been confirmed that the D/W pressure increase for some reason was not able to explain the measured PCV pressures. Therefore, by the process of elimination, the cause of the PCV pressure increase should be explored on the S/C side.

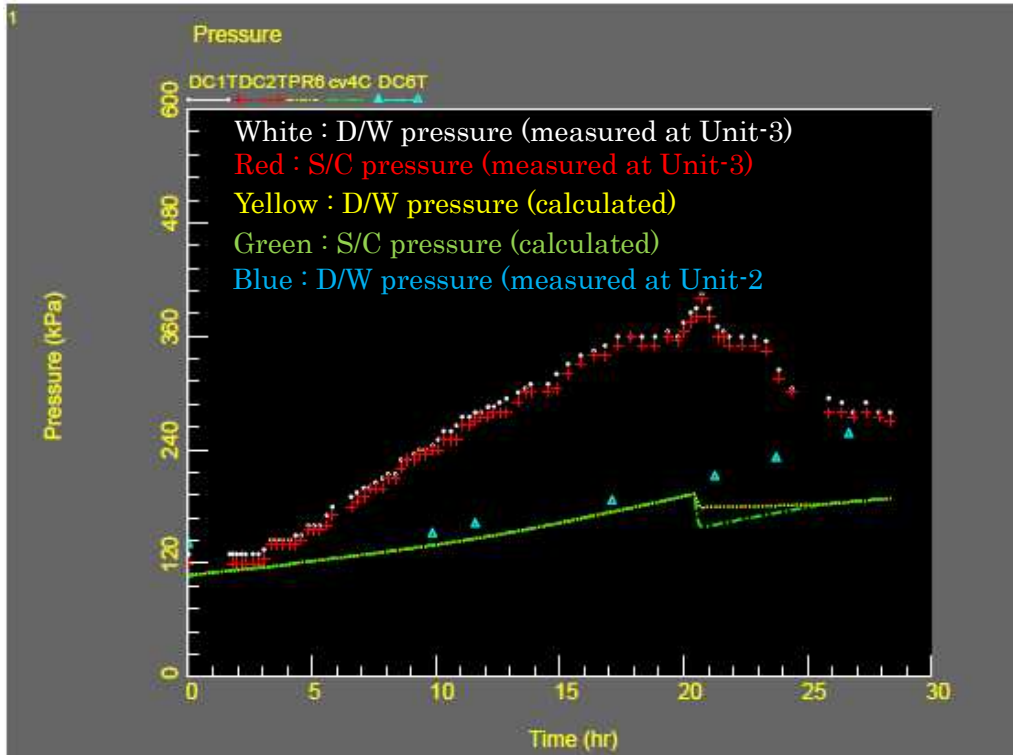


Figure 3-3 PCV pressure (Case 1)

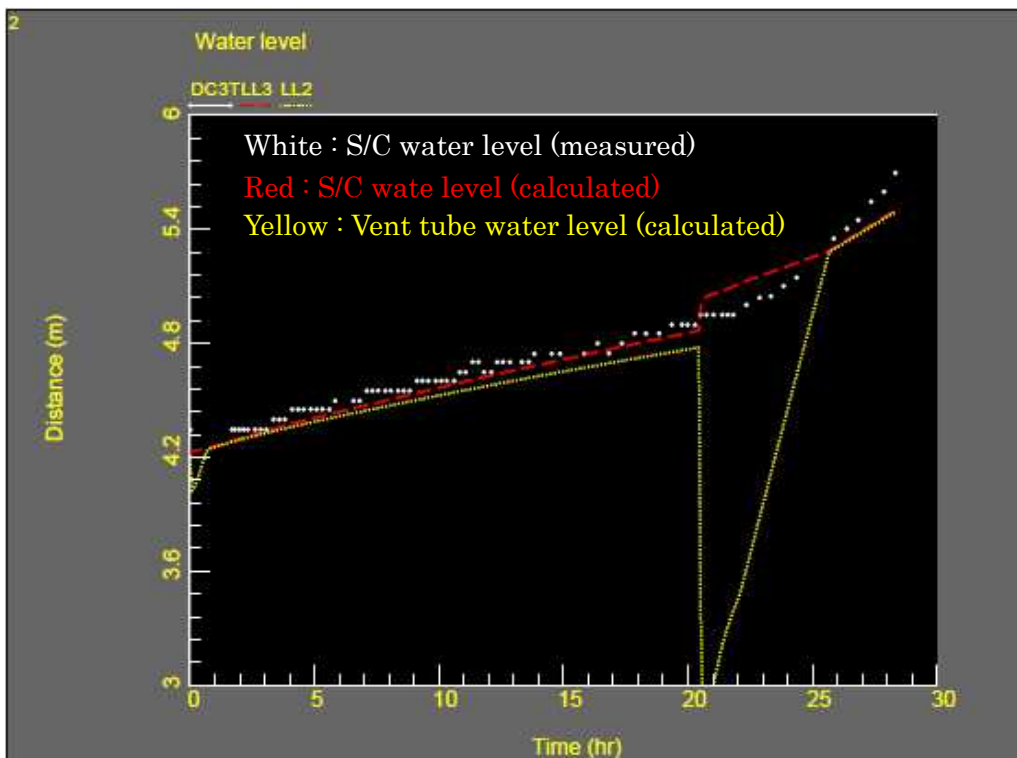


Figure 3-4 S/C water level and vent tube water level (Case 1)

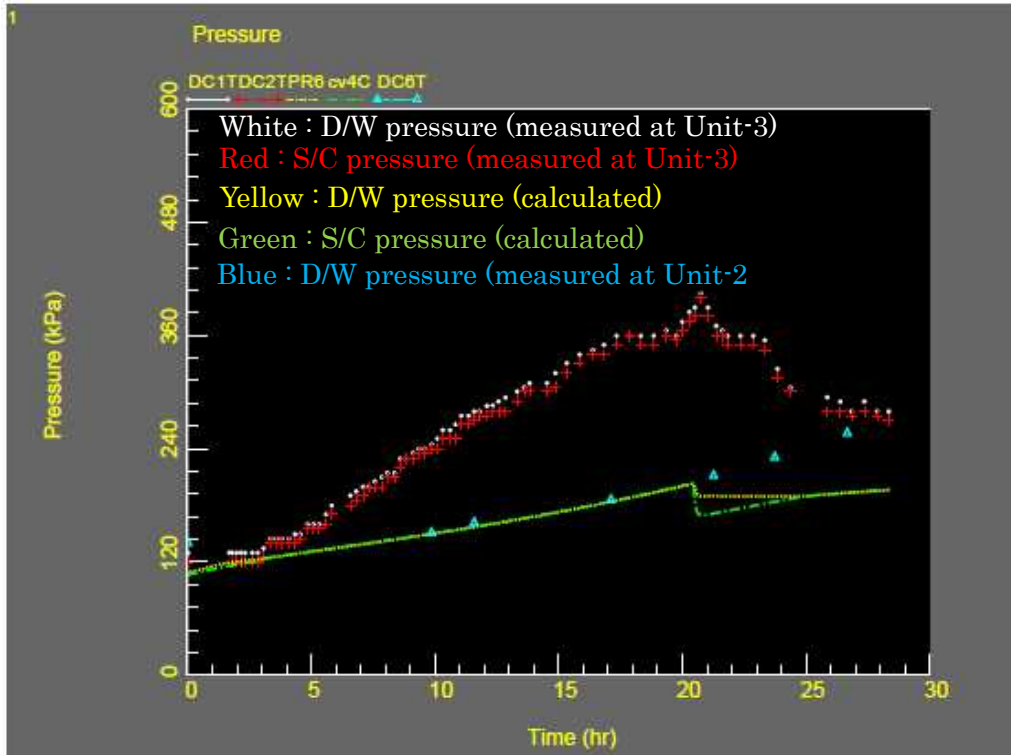


Figure 3-5 PCV pressure (Case 2)

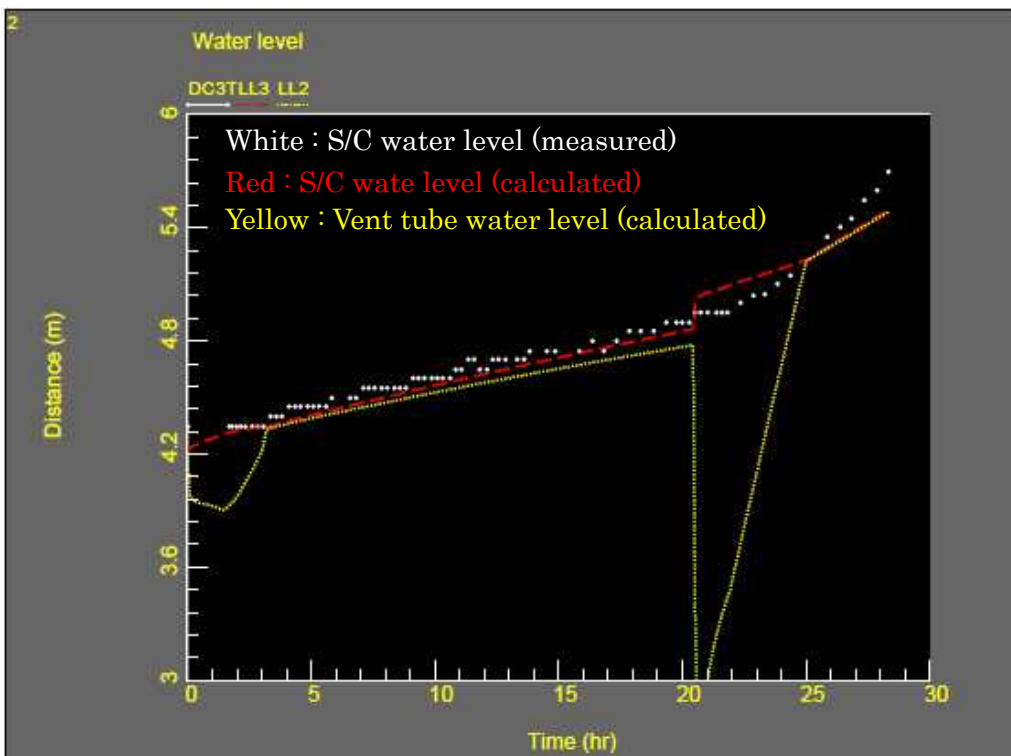


Figure 3-6 S/C water level and vent tube water level (Case 2)

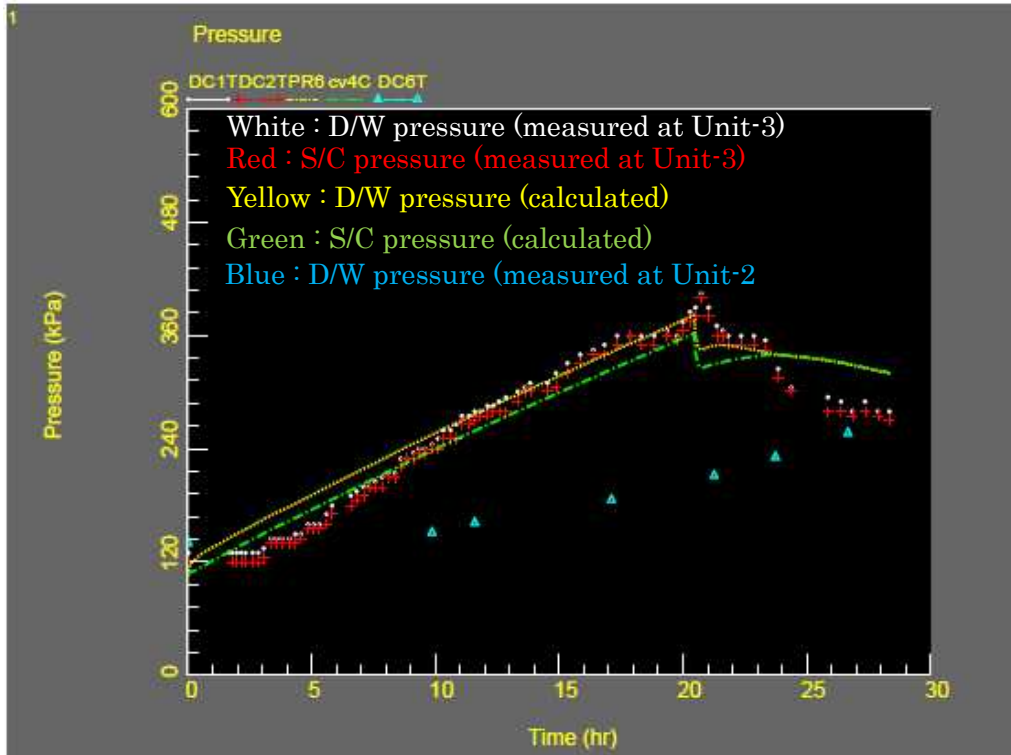


Figure 3-7 PCV pressure (Case 3)

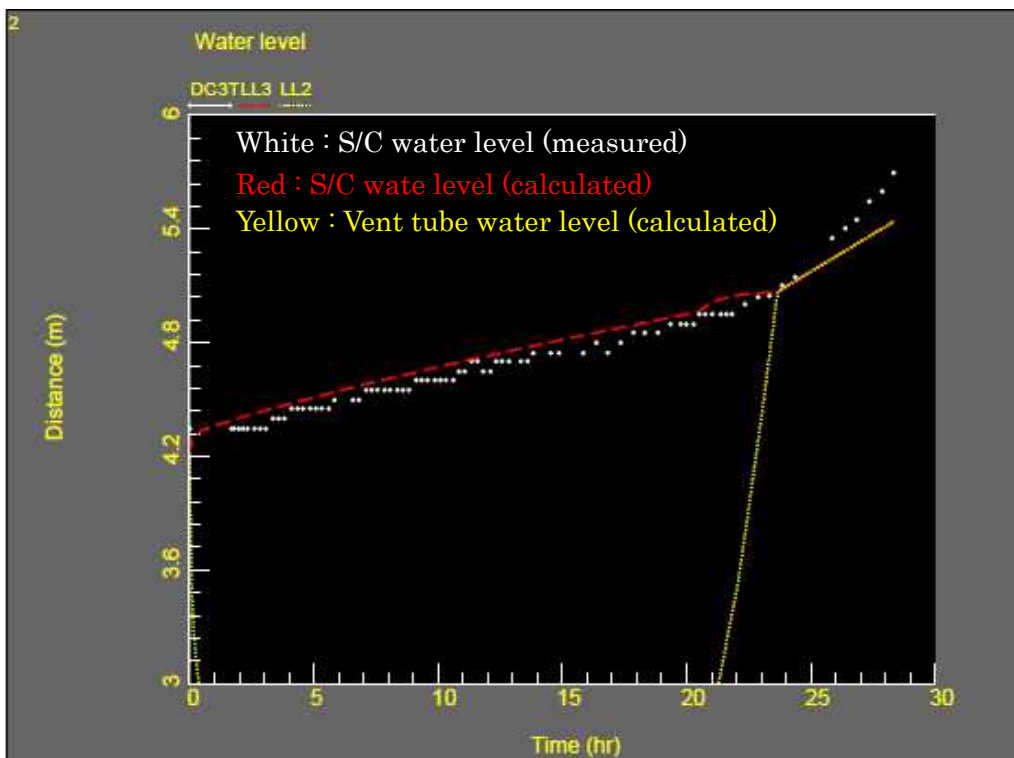


Figure 3-8 S/C water level and vent tube water level (Case 3)

4. Literature survey on the S/C thermal stratification

Based on an elimination process for candidate causes, the PCV pressure behavior obtained by the analysis in Section 3 indicated that the cause of the pressure increase might have been on the S/C side. Thermal stratification is a possible factor on the S/C side to cause the PCV pressure increase. In this connection, this section examined the possibility of thermal stratification being formed in the S/C pool, based on a relevant literature survey on the effects of exhaust steam from the RCIC and SRVs on the S/C temperature distribution.

4.1. Tests simulating RCIC operation

Figure 4-1 illustrates the RCIC exhaust outlet structure. A vertical pipe forms the outlet (sparger) with its bottom end blocked and alternately arranged window holes on the wall, through which the exhaust steam is discharged horizontally to the pool. The diameter of the holes is small on the upper part and large on the lower part.

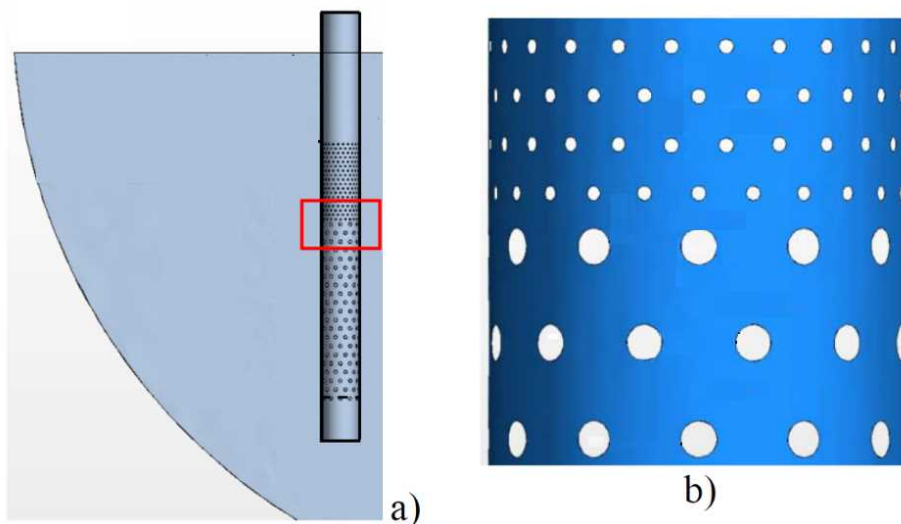


Figure 4-1 Structure of RCIC sparger of Unit-3 [5]

Steam discharge tests were carried out in the reported study [5] using a pipe simulating an RCIC sparger of Unit-3 in order to see the condensing behavior of the steam discharged horizontally from the sparger and its effects on the temperature distributions in the pool. Figure 4-2 shows the test configuration. The sizes of the discharge windows (holes) were the same as the actual ones and the steam discharge rate per unit area was made equal to that of the actual values by setting the number of discharge windows and steam flow rate at about 1/24 of the actual values. The discharge windows were positioned about 80cm to 280cm below the surface for a water pool of 300cm depth and 65cm by 65cm width. The pool was

not sealed and open to the air throughout the entire test time. Twelve thermometers were located at 20cm intervals in the pool at depths between 40cm and 260cm to measure temperatures at each elevation upon steam discharge.

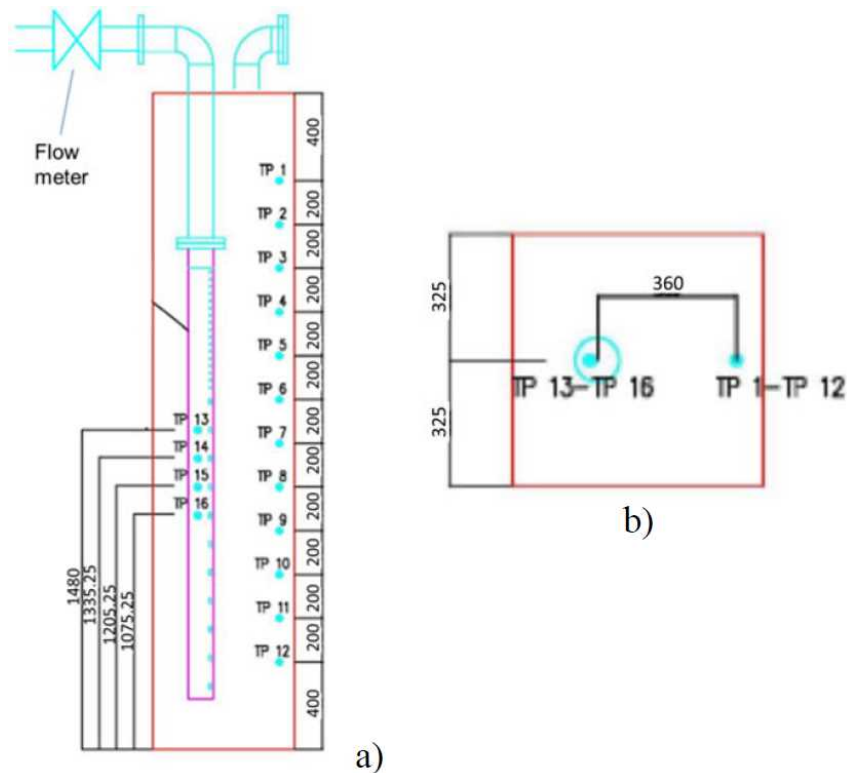


Figure 4-2 Test geometry for simulating RCIC [5]

Figure 4-3 shows the test results. For about the first 10 minutes the pool temperature increased uniformly. In the tests, a phenomenon called “chugging” was repeated, resulting in the pool water being stirred and the temperatures being homogenized (chugging describes high frequency, small scale water hammers; this behavior occurs when bubbles are condensed near the outlet holes, the pressure drops locally, amounts of water are sucked into the tube, the condensation is accelerated, and the water is discharged violently thereafter). Generally, this chugging occurs more often when the pool temperature is lower, the flow rate per unit area is lower and the discharge holes are larger. When the pool temperatures were increased to a certain level, the chugging stopped and thereafter TP12, TP11 and TP10 in the lower part of the pool showed lower temperatures than the other thermometers, which meant thermal stratification was being formed in the pool. Once chugging stopped, steam discharged from the windows (outlet holes) condensed in a stable manner in the pool, the water warmed by the steam went upward due to buoyancy, and

relatively cold water returned instead to the area of the outlet holes from above, thus forming a water circulating path (high temperature layer) in the upper part of the pool. When the pool water temperatures in the upper part reached the saturation temperature thereafter, readings at TP10, TP11 and TP12 increased one after another. This happened because the steam that was discharged from the holes was going upward without condensing and it formed an upward force on the surrounding water, thus intensifying the above-mentioned circulating water in the upper part of the pool, and this high temperature layer extended to the lower part of the pool.

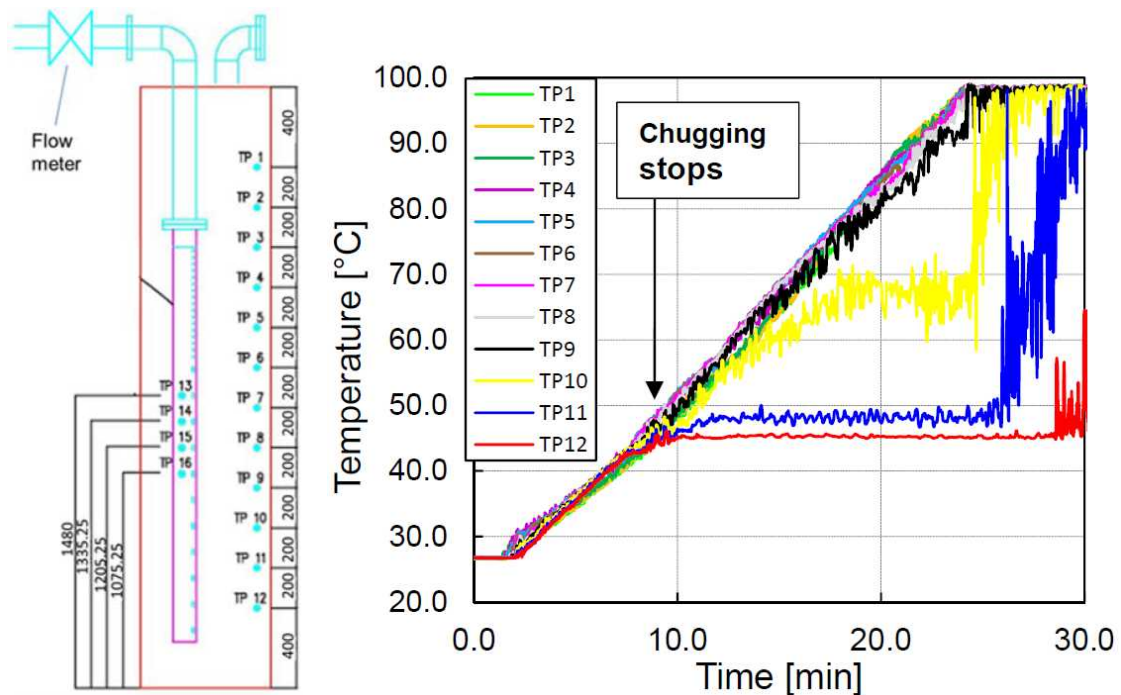


Figure 4-3 Results of RCIC simulation test [5]

The temperature profiles of the S/C pool water during the RCIC operation at Unit-3 were estimated based on the test results above. The thermal stratification observed in the test can be considered to occur in the actual reactor, too, because the test used the same diameters of steam discharge holes and the flow rate per unit area.

While the S/C pool water temperatures were low, the pool water could have been stirred by chugging. But, as a matter of fact, the RCIC piping of the actual reactor was equipped with a check valve to prevent pressure decrease in the pipe. Therefore, chugging effects in the actual system would have been less than in the test.

On the other hand, once the pool water temperatures in the upper part reached about the saturation temperature, the high temperature water layer would have extended to the lower

part as estimated in the test. But the extending speed in the actual reactor would have been less than in the test. Two reasons can be considered for this estimation. One is that the water inventory in the S/C pool was much larger than that of the test loop, more than 2,000 times, and a longer time was needed for the upward force given to water by the steam to influence the whole water circulation in the pool. The other reason is that, while the test loop was an open system, the actual system was a closed system being combined with the D/W. Consequently, when the surface water temperatures increased, the saturation temperature also increased and therefore the fraction of uncondensed steam would have become less than in the test.

From the above, thermal stratification would have been formed in the S/C pool when the RCIC was in operation and the water stirring effects (chugging) observed in the test loop would have been more than in the actual case.

4.2. Tests simulating SRV operation

The Monticello, a reactor which has a torus-type suppression chamber and SRV exhaust outlet (T-quencher) similar to those of Unit-3, was used in the test. A test series [6] was conducted to measure the temperature profile in the S/C pool when an SRV was in service. The temperatures at various points in the S/C were measured in the test when a single SRV was kept open for about 11 minutes.

Figure 4-4 shows the structure of the SRV T-quencher used in the test. The SRV exhaust steam flowed to the "ARMS" via the "SRV DISCHARGE LINE" and was discharged to the pool through a number of horizontally arranged outlet holes. The discharge outlets were also on the opposite side (the "SRV DISCHARGE LINE" side) and the steam was discharged from both ARM sides. The T-quencher in the figure had an open hole at the tip of "ARM 2" (the right leg in the figure), one of the differences from the actual system of Units-2 and -3, but it was basically similar to the actual system structure.

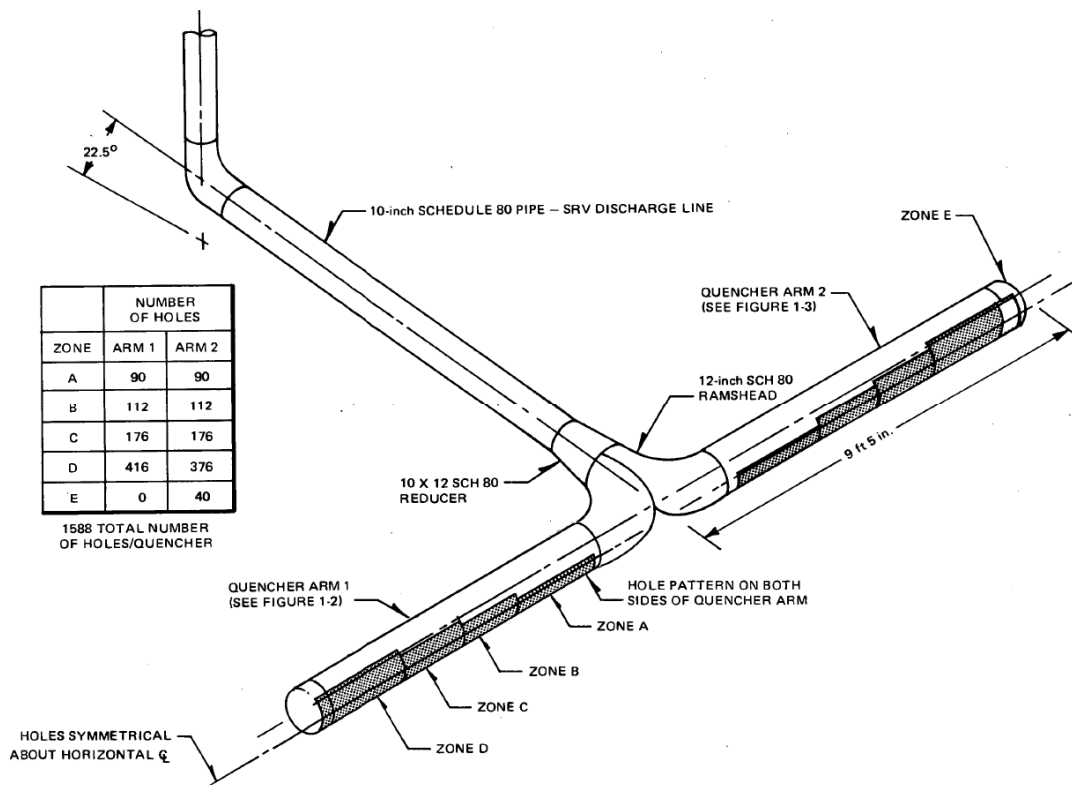


Figure 4-4 Structure of SRV T-quencher used in the test [6]

Figure 4-5 shows the layout of the SRV T-quencher in the S/C in the test. Steam was discharged from the T-quencher “D” in top right in the figure for 667s. The steam flow rate per second was set at the rated flow rate of the Unit-3 SRV. The initial pool water temperature was about 10 deg C and the pool water inventory was about 2,000m³ (about two-thirds of the inventory of Unit-3).

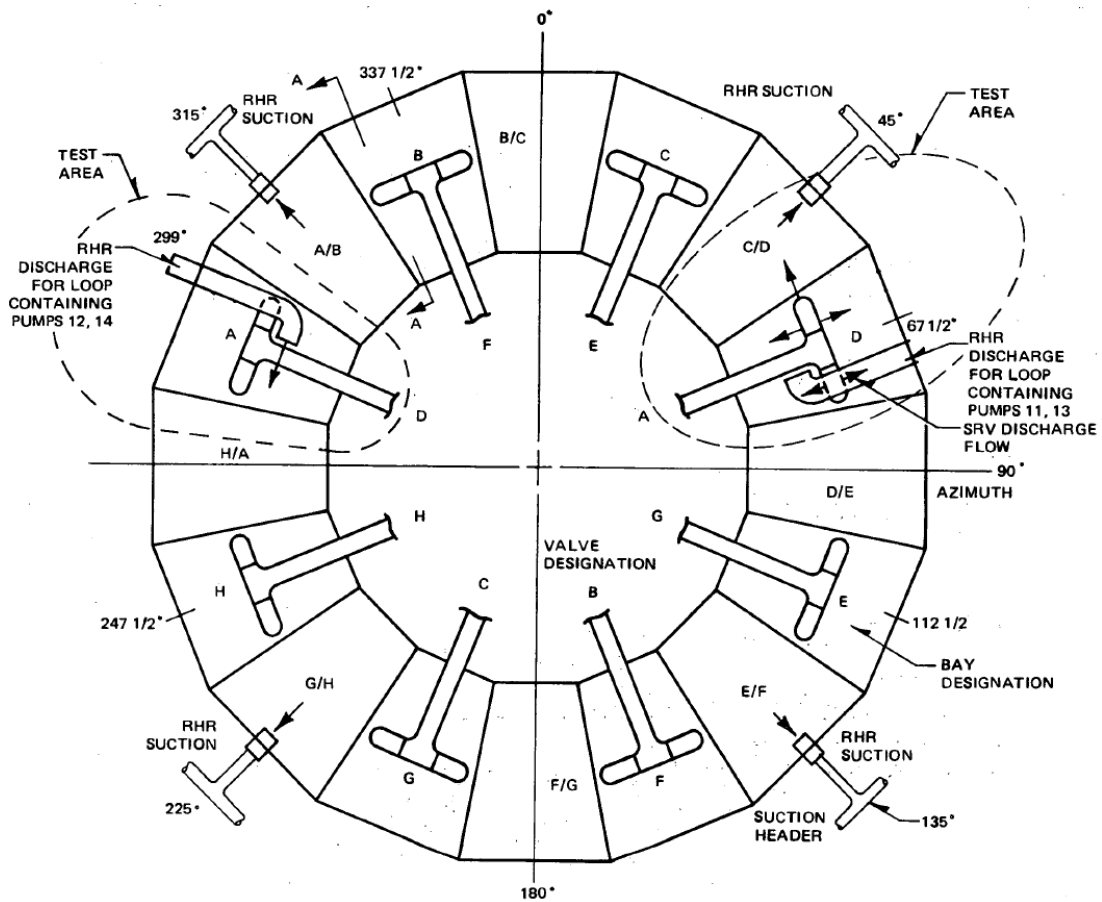


Figure 4-5 Layout of SRV T-quenchers in the test [6]

Schematic illustrations explaining the results are shown in Figure 4-6, which was created based on the radial distribution of temperatures measured and averaged in the vertical direction cited from the test report [6] and a summary report of the test [7]. The detailed numerical data of the vertical profile of measured temperatures have not been made public. The circumferential cross section in Figure 4-6 is the cross section of the torus-type S/C in Figure 4-5 being cut open along the circle enveloping the steam outlets of the T-quenchers A to H, when viewed horizontally. During the measurements, the initial temperature value was maintained almost the whole time in the lower part of the pool except just below the SRV T-quenchers, while the water temperatures in the upper part were relatively higher. The results indicated the possibility that the pool surface water temperatures became higher when the SRVs were operated.

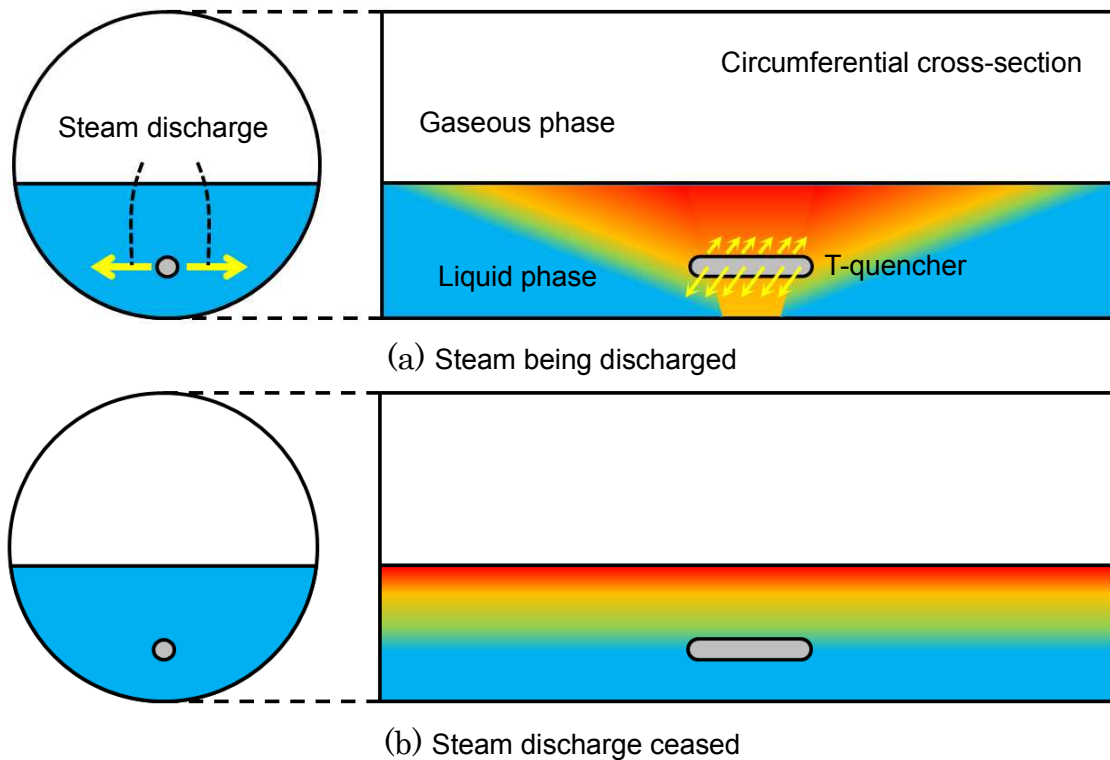


Figure 4-6 Schematic illustrations of temperature profile in the S/C pool in the test

The temperature profiles of the S/C pool water during the SRV operation at Unit-3 were estimated based on the above test results. The test was conducted on the actual plant with a similar configuration to the Unit-3 PCV. Therefore, the S/C pool of Unit-3 is anticipated to have high temperature water on its surface and thermal stratification, too, assuming the same SRV operating conditions in the test.

However, there remain some unknown operation conditions for the SRVs of Unit-3. As was shown in Figure 2-1, the RPV pressures before HPCI operation on March 12th exceeded the SRV working pressures intermittently and this suggests that the SRVs worked, but which SRV out of 8 worked is unknown and the duration of its operation or steam flow rates are unknown. Therefore, it is not clear as of now whether thermal stratification occurred in the S/C pool of Unit-3 as was the case in the test.

Furthermore, the chart data (Figure 4-7 [4]) of S/C temperatures of Unit-2 before the tsunami arrival showed that the temperatures increased over a wide circumferential region. In addition, the measured temperatures were increasing in disorder. This suggests the stirring effects of SRV exhaust. Consequently, the effect of thermal stratification formed by SRV operations is considered less when compared with that of RCIC operations.

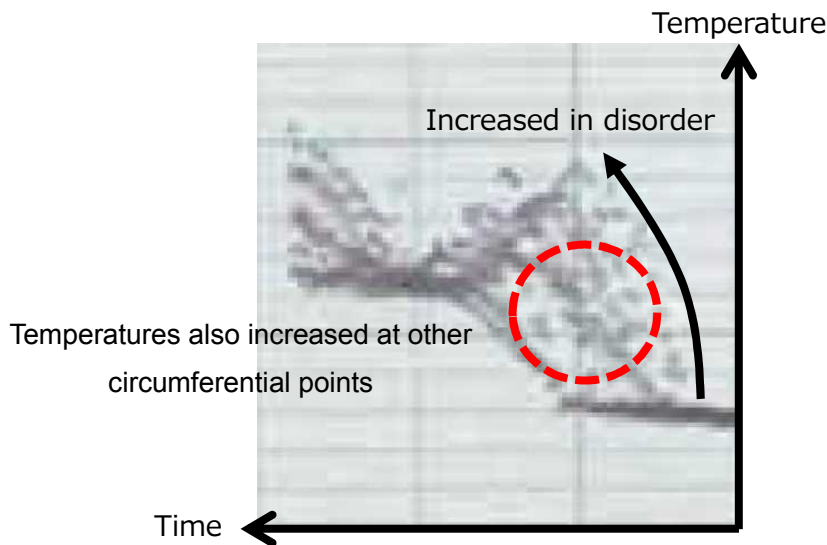


Figure 4-7 S/C pool water temperatures of Unit-2 before tsunami arrival [4]

4.3. Estimation of the causes of PCV pressure increase based on the literature survey

When the effects of RCIC exhaust and SRV exhaust on the S/C thermal stratification are taken into account, the effect by the RCIC operation is considered significant, since the RCIC of Unit-3 was being continuously operated, not intermittently in the usual mode. Furthermore, the exhaust flow rate of the SRVs was less than the usual rate because of the RCIC continuous operation and thus the S/C pool water is considered to have been less stirred by the SRV exhaust than in the test referred to. Consequently, thermal stratification would have developed in the S/C pool water, accelerating the PCV pressure increase.

5. Measures taken at the Kashiwazaki-Kariwa NPS to response to thermal stratification

The following measures have been incorporated in the accident management procedures at the Kashiwazaki-Kariwa NPS: (i) the S/C pool water is to be directly cooled by the residual heat removal system or spray on the S/C; or (ii) the S/C pool water temperatures are to be controlled to increase uniformly by activating SRVs, which are distributed in the whole S/C pool; the activation occurs in the order of one after another, and is mutually independent of each other, while monitoring the S/C pool temperatures. The reliability of these measures are being reinforced by “strengthening of power supply systems,” “installing stand-by heat exchangers” and other means.

6. Conclusion

Examination was conducted into the causes of the faster than anticipated PCV pressure increase from March 11th to 12th of Unit-3 from the decay heat. The following points were clarified.

, Based on the measured values at the time of the accident, an attempt was made to identify the causes of the PCV pressure increase. The measured pressure difference between the D/W pressure and S/C pressure was not in agreement with the pressure difference anticipated for either the D/W or the S/C being the cause of the PCV pressure increase. It was not possible to identify, from the measured values, whether the cause of the PCV pressure increase had existed in the D/W or the S/C.

The PCV pressure behavior was investigated by analysis when leaks were assumed to have occurred from the RPV to the D/W. The results showed that large leaks from the RPV to the D/W could reproduce the PCV pressure increasing behavior up until the time of S/C spray, but not to reproduce the PCV pressure decreasing behavior after the S/C spray. Therefore, by a process of elimination, the cause of the PCV pressure increase should be explored on the S/C side.

Meanwhile, an investigation was conducted based on a literature survey concerning the effects of exhaust from the RCIC and SRVs on the S/C pool water thermal stratification. It was found that the occurrence of thermal stratification might have been accelerated during the RCIC operation but the contribution of SRV operations to the occurrence of thermal stratification might have been less. Since the RCIC of Unit-3 was being continuously operated, not intermittently in the usual mode, the contribution of the RCIC exhaust is considered to be bigger in forming thermal stratification, and since the exhaust flow rate of the SRVs was less than the usual rate, the occurrence of thermal stratification would have been accelerated in the S/C pool water.

A high likelihood can be concluded from the above results that the thermal stratification in the S/C pool water was the main cause of the PCV pressure increase at Unit-3 faster than anticipated from the decay heat.

For further in-depth investigation, thermal-hydraulic analysis codes for the PCV will be used to evaluate quantitatively the temperature distributions in the S/C pool.

7. References

- [1] JNES, Study on the impacts on the PCV pressures and other plant data by thermal stratification of the S/C pool water, February 1, 2012 (in Japanese)

- [2] Information Portal for the Fukushima Daiichi Accident Analysis and Decommissioning Activities
<https://fdada.info/index>
- [3] Tokyo Electric Power Company, Inc., Unit-3 plant data readings at the Great East Japan earthquake, August 6, 2014
- [4] Tokyo Electric Power Company, Inc., The Impact of Tohoku-Chihou Taiheiyo-Okai Earthquake to Nuclear Reactor Facilities at Fukushima Daiichi Nuclear Power Station, May 9, 2012 (in Japanese)
- [5] M. Pellegrini, Suppression pool testing at the SIET labs (3) Experiments on Steam Direct Contact Condensation in a Vertical Multi-hole Sparger, 2014/12
- [6] Patterson, BJ, Mark I Containment Program, Monticello T-Quencher Thermal Mixing Test, Final Report, NEDO-24542, 1979/8
- [7] U.S. NRC, Suppression Pool Temperature Limits for BWR Containments, NUREG-0783, 1981

(End)